Dual PI3K/mTOR Inhibition Suppresses Tumor pO_2 within Viable Tumor Assessed by ^{19}F-MRI and Multispectral Analysis

Yunzhou Shi[1], Jason Oeh[2], Jeffrey Eastham-Anderson[3], Sharon Yee[2], David Finkle[2], Franklin V. Peale[3], Jed Ross[1], Maj Hedehus[1], Nicholas van Bruggen[1], Rayna Venook[2], Sarajane Ross[2], Deepak Sampath[2], and Richard A. D. Carano[1]

[1]Biomedical Imaging, Genentech Inc.(Roche Group), South San Francisco, CA, United States, [2]Translational Oncology, Genentech Inc.(Roche Group), South San Francisco, CA, United States, [3]Pathology, Genentech Inc.(Roche Group), South San Francisco, CA, United States

Introduction. The phosphoinositide 3-kinase (PI3K)/mammalian target of rapamycin (mTOR) pathway is a key signaling pathway in human cancer [1]. The inhibition of this pathway is known to block tumor cell growth and inhibit tumor angiogenesis [1]. GDC-0980, a novel dual inhibitor of mTOR and PI3K, has been shown to have potent anti-vascular effects, suppressing vascular density and function due to PI3K's role in vascular endothelial growth factor (VEGF) receptor 2 intracellular signaling [2]. The effect of dual PI3K/mTOR inhibition on tumor oxygen level, however, remains unknown since the inhibitor reduces both tumor cell metabolism (O_2 consumption) and vascular function (O_2 supply). Previously, we developed a novel approach that combines ^{19}F MRI T_1 mapping with diffusion-based multispectral K-means clustering to quantify pO_2 in specific tumor tissue populations [3]. The current study aims to elucidate the role of PI3K/mTOR signaling on oxygen level in viable tumor by using an *in vivo* multispectral ^{19}F-MRI approach. An anti-angiogenic agent, B20.4.1.1, which blocks both murine and human VEGF, is employed as a positive control for its known anti-vascular effects.

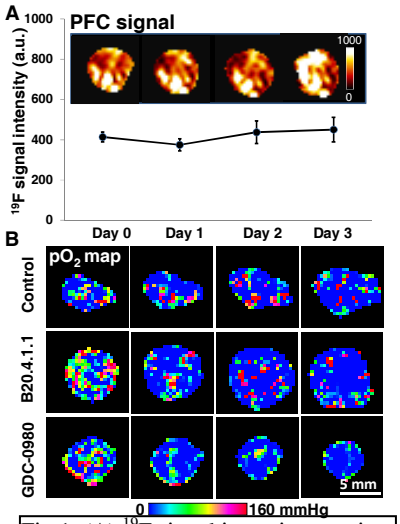

Fig.1. (A) ^{19}F signal intensity remains stable. Representative tumor slice during 4 days. (B) Representative pO_2 maps from each group from day 0 to day 3 (left to right).

Methods. MR experiments: Experiments were performed with a 9.4T Agilent MRI system equipped with a ^{1}H/^{19}F 10 mm surface coil (Agilent Technologies Inc.). 1-mm-thick coronal slices were acquired (n = 12, FOV=25.6×25.6mm, matrix=64×64). A diffusion-weighted fast spin echo multislice (FSEMS) sequence was used to calculate an apparent diffusion coefficient (ADC) map (6 b-values ranging from 270 to 1000 s/mm^2, TR=3s, ETL=4, NA=2, Δ=30ms, δ=3.3ms). A spin echo multislice (SEMS) sequence was used to generate T_2 and M_0 maps (TE = 5,26,47,68 ms, TR = 3s, NA= 1). A T_1-weighted SEMS sequence was used to obtain a fluorine anatomical reference image (TR=5s,TE=8.5ms,NA=4). A ^{19}F single-shot, inversion recovery FSEMS sequence was employed to generate spatial maps of T_1 (FSEMS, TI =0.1,0.3,0.5,0.6,0.7,0.9,1.2,1.8,2.5s, TR=6s, ESP=4.1ms, ETL=32, NA=32, matrix=32×32, zero-filled to 64 ×64). Multispectral analysis of ^{1}H data was used for tissue segmentation. K-means clustering was performed using the ADC, proton density and T_2 maps as previously described [3]. The K-means algorithm segmented the tumors into four tissue classes: viable tumor tissue, sub-cutaneous adipose tissue, and two necrotic classes [3]. The tissue class map was combined with the ^{19}F T_1 map to estimate pO_2 in the four tissue classes.

Samples and animals: The Institutional Animal Care and Use Committee at Genentech approved all animal protocols. Athymic nude mice (n=30) were inoculated subcutaneously on the hind limb with HM7 colorectal cancer cells. The imaging contrast agents, PFCs containing 60 w/v% perfluoro-15-crown-5-ether (Synquest Inc.) were intravenously injected into mice (400 µL/dose) at 48 h and 24 h prior to MRI, respectively. Imaging was performed on day 0, day 1, day 2 and day 3, respectively. B20.4.1.1 (10mg/kg, n=10) was administered as a single iv dose on day 0. GDC-0980 (10 mg/kg, n=10) was administered orally on days 0, 1 and 2. Anti-ragweed IgG and 0.5% methycellulose/0.2% Tween 80 (MCT) were used as control (n=10) for B20.4.1.1 and GDC-0980, respectively. A second proof-of-concept study was carried out between B20.4.1.1 treatment (n=13) and anti-ragweed control (n=11) for 24 h.

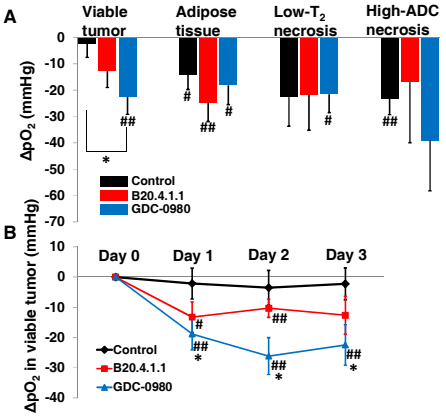

Fig.2. (A) Mean ΔpO_2 (day 3-day 0) in four tissue classes. (B) Mean ΔpO_2 change in viable tumor (with std error). * p<0.05 vs control. # p<0.05, ## p<0.01 vs pre-tx.

Results and Discussions. PFC remained in the tumor throughout the course of study following intravenous injection. No significant loss of ^{19}F signal was observed (Fig.1A), which enabled longitudinal study of pO_2 change. Similar to our previous study [3], the pO_2 maps were quite heterogeneous (Fig. 1B). After treatments, there was a heterogeneous response in different tumor tissue classes (Fig. 1B, 2A). In general, both the B20.4.1.1 and GDC-0980 groups decreased pO_2 in viable tumor post-treatment relative to pre-treatment levels, with GDC-0980 having a strong effect for all 3 days post-treatment (Fig. 2B). When compared with the control group, the GDC-0980 group exhibited a significant decrease in pO_2 (p<0.05), while the B20.4.1.1 group showed a trend towards a reduction of pO_2 (p=0.14). In the second proof-of-concept study, the B20.4.1.1 group showed a significant reduction of pO_2 within 24 h in comparison with control (Control: -4.27±5.52, B20.4.1.1: 18.78±3.92, p<0.05). Taking the results together, there appears to be variability in pO_2 response after B20.4.1.1 treatment. The strong suppression of pO_2 induced by GDC-0980 is likely due to the suppression of oxygen supply due to the loss of small functional vessels as previously demonstrated by VSI MRI [2]. In addition, compared to B20.4.1.1, an anti-VEGF-A mono therapy, GDC-0980 treatment resulted in greater tumor growth inhibition due to both PI3K pathway inhibition in the tumor cells and a strong anti-vascular effect (data not shown).

Conclusions. The current results demonstrate that PI3K/mTOR inhibition strongly suppresses tumor oxygenation. In addition, these results advocate for the use of the multispectral ^{19}F-MRI technique as a tool to better understand the mode of action of therapies that alter tumor's microenvironment.

References [1]Liu *et al*., Nature Reviews 2009. [2] Wyatt *et al*., ISMRM 2011, p759. [3] Shi *et al*., ISMRM 2012, p167.